

Numerical evaluation of the tensor bispectrum in two field inflation

Rathul Nath Raveendran and L. Sriramkumar

^aThe Institute of Mathematical Sciences, HBNI, CIT Campus, Chennai 600113, India

^bDepartment of Physics, Indian Institute of Technology Madras, Chennai 600036, India

E-mail: rathulnr@imsc.res.in, sriram@physics.iitm.ac.in

Abstract. We evaluate the dimensionless non-Gaussianity parameter h_{NL} , that characterizes the amplitude of the tensor bispectrum, *numerically* for a class of two field inflationary models such as double inflation, hybrid inflation and aligned natural inflation. We compare the numerical results with the slow roll results which can be obtained analytically. In the context of double inflation, we also investigate the effects on h_{NL} due to curved trajectories in the field space. We explicitly examine the validity of the consistency relation governing the tensor bispectrum in the squeezed limit. Lastly, we discuss the contribution to h_{NL} due to the epoch of preheating in two field models.

Contents

1	Introduction	1
2	Background equations	3
3	The tensor modes and the power spectrum	4
4	The tensor bispectrum and the corresponding non-Gaussianity parameter	5
5	The non-Gaussianity parameter h_{NL} in slow roll inflation	7
6	Numerical evaluation	7
6.1	Double inflation	8
6.2	Hybrid inflation	11
6.3	Aligned natural inflation	11
7	Consistency relation in the squeezed limit	12
8	The contribution during preheating	14
9	Discussion	14

1 Introduction

In the absence of equally effective alternatives, the inflationary paradigm continues to remain the most compelling scenario to describe the origin of perturbations in the primordial universe. Inflation—which refers to a period of accelerated expansion during the early stages of the radiation dominated epoch—was initially proposed to explain cosmological observations such as the extent of homogeneity and spatial flatness of the universe. However, soon after the original proposal, it was realized that apart from helping to overcome the drawbacks of the conventional hot big bang model, the inflationary scenario also provides a causal mechanism for the generation of primordial perturbations. According to the inflationary paradigm, the primordial perturbations are generated due to quantum fluctuations, which are rapidly stretched to cosmological scales due to the accelerated expansion. The perturbations generated during inflation lead to anisotropies in the Cosmic Microwave Background (CMB), which in turn result in the large scale structure of galaxies and clusters of galaxies that we see around us today (see, for instance, any of the following reviews: Refs. [1–7]).

Typically, the period of accelerated expansion is assumed to be driven by scalar fields. Many models consisting of single and multiple scalar fields have been proposed to achieve inflation. The potentials governing the scalar fields, along with the values of the parameters describing them, determine the dynamics during inflation. It is the quantum fluctuations associated with the scalar fields that are responsible for the primordial perturbations. The background inflationary dynamics determines the characteristics of these perturbations, which are conveniently described in terms of correlation functions. The CMB and other cosmological data point to a nearly scale invariant primordial scalar power spectrum as is

generated by the simplest models of slow roll inflation [8–16]. However, despite the strong constraints that have emerged, there exist many inflationary models that are consistent with the data at the level of two-point functions. In the case of canonical single field models, there has been a comprehensive comparative analysis of a fairly large set of models with the cosmological data [11–16]. Clearly, in the long run, it would be desirable to carry out a similar comparison of multi field models and, more specifically, two field models with the data (see, for instance, Refs. [16–19]). As far as the background evolution is concerned, two field models offer a richer dynamics than the single field models due to the possibility of different types of trajectories in the field space. At the level of perturbations, the existence of iso-curvature perturbations in multi field models can lead to a non-trivial evolution of the curvature perturbation on super-Hubble scales (see, for example, the following articles [20–26] or reviews [27–29]).

Over the last decade and a half, it has been recognized that observations of primordial non-Gaussianities—in particular, the amplitude of three-point functions—can help us arrive at a smaller class of viable inflationary models. This expectation has been corroborated to a large extent by the strong constraints that have been arrived at by the Planck data on the three non-Gaussianity parameters that describe the amplitude of the scalar bispectrum [30]. Theoretically, a considerable amount of work that has been carried out towards understanding the non-Gaussianities generated in single and multi field inflationary models. However, the theoretical understanding of non-Gaussianities generated in inflationary models and the observational constraints that have been arrived at are largely concentrated on the scalar bispectrum and the corresponding non-Gaussianity parameters [31–52].

In fact, apart from the scalar bispectrum, there arise three other three-point functions when the tensor perturbations are also included [53–56]. The three-point functions are often evaluated analytically in the slow roll approximation, and one has to resort to numerical efforts to evaluate these three-point functions in a generic situation (in this context, see, for instance, Refs. [56–63]). Also, while numerical procedures have been developed to evaluate the three-point functions in single field models [56–63], until very recently, there has been little effort towards computing these quantities in multi field models. As we were converging on the manuscript, there appeared three coordinated efforts wherein the scalar bispectrum has been numerically evaluated in multi field models [64–66]. While these efforts are indeed more comprehensive and focus on the important case of scalars, the approach adopted in these efforts (the so-called transport method) is different from the method we work with. Our eventual goal is to arrive at a numerical procedure to evaluate all the three-point functions in two field and, in general, multi field models. In contrast to the scalars, the tensor perturbations are simpler to study as they depend only on the evolution of the scale factor. As a first step of the process, in this work, we compute the tensor bispectrum and the corresponding non-Gaussianity parameter in two field models of inflation. To check the accuracy of the numerical procedure, we first consider simple situations leading to slow roll inflation and compare the numerical results with the analytical results available in such cases. We then study the effects of the curved trajectory in the field space on the tensor bispectrum and the corresponding non-Gaussianity parameter. We also explicitly examine the validity of the consistency relation governing the three-point function in the squeezed limit and discuss the contributions to tensor non-Gaussianities during the epoch of preheating.

This paper is organized as follows. In the following section, we shall quickly summarize the equations of motion describing the background dynamics of inflationary scenarios driven by two canonical scalar fields. In Sec. 3, we shall outline the quantization of the tensor modes

and the definition of the tensor power spectrum. In Sec. 4, we shall present the essential expressions governing the tensor bispectrum arrived at using the Maldacena formalism and introduce the dimensionless non-Gaussianity parameter h_{NL} that characterizes the amplitude of the tensor bispectrum. In Sec. 5, we shall discuss the analytical results for the tensor bispectrum and the corresponding non-Gaussianity parameter in the de Sitter limit. In Sec. 6, we shall describe the numerical procedure that we adopt to calculate the tensor bispectrum and the non-Gaussianity parameter and then go on to evaluate these quantities in three different two field models, *viz.* double inflation, hybrid inflation and aligned natural inflation. Moreover, in the case of double inflation, we study the imprints of turning trajectories on h_{NL} . In Sec. 7, using our numerical techniques, we also examine the so-called consistency condition relating the tensor bispectrum to the tensor power spectrum in the squeezed limit, wherein one of the wavenumbers involved is much smaller than the other two. In Sec. 8, we shall discuss the effects of preheating on the non-Gaussianity parameter h_{NL} . Lastly, in Sec. 9, we shall conclude with a brief summary.

Note that, we shall work with natural units wherein $\hbar = c = 1$, and define the Planck mass to be $M_{\text{Pl}} = (8\pi G)^{-1/2}$. We shall adopt the metric signature of $(-, +, +, +)$. As usual, overdots and overprimes shall denote differentiation with respect to the cosmic and the conformal time coordinates, respectively. Also, N shall refer to the number of e-folds.

2 Background equations

We shall consider the background to be the spatially flat, Friedmann-Lemaître-Robertson-Walker (FLRW) metric that is described by the line-element

$$ds^2 = -dt^2 + a^2(t) \delta_{ij} dx^i dx^j = a^2(\eta) (-d\eta^2 + \delta_{ij} dx^i dx^j), \quad (2.1)$$

where the quantity a denotes the scale factor, while t and $\eta = \int dt/a(t)$ represent the cosmic and the conformal time coordinates. We shall study inflationary models consisting of two scalar fields, say, ϕ and χ , that are described by the action

$$\mathcal{S}[\phi_I] = \int d^4x \sqrt{-g} \left[-\frac{1}{2} \sum_{I=1}^2 \partial_\mu \phi_I \partial^\mu \phi_I - V(\phi_I) \right], \quad (2.2)$$

where $\phi_I = \{\phi, \chi\}$ and $V(\phi_I)$ is the potential characterizing the scalar fields. The equations of motion that govern the homogeneous components of these scalar fields are given by

$$\ddot{\phi}_I + 3H \dot{\phi}_I + V_I = 0, \quad (2.3)$$

where $V_I = \partial V / \partial \phi_I$. The quantity $H = \dot{a}/a$ denotes the Hubble parameter and its evolution is described by the following Friedmann equation:

$$H^2 = \frac{1}{3M_{\text{Pl}}^2} \left[\frac{1}{2} \sum_{I=1}^2 \dot{\phi}_I^2 + V(\phi_I) \right]. \quad (2.4)$$

It is useful to introduce here the so-called first slow roll parameter ϵ_1 , which is defined as

$$\epsilon_1 = -\frac{\dot{H}}{H^2}. \quad (2.5)$$

3 The tensor modes and the power spectrum

As we have mentioned earlier, we shall be focusing on the tensor perturbations in this work. When the tensor perturbations are taken into account, the FLRW metric can be expressed as [31]

$$ds^2 = a^2(\eta) \left\{ -d\eta^2 + \left[e^{\gamma(\eta, \mathbf{x})} \right]_{ij} dx^i dx^j \right\}, \quad (3.1)$$

where γ_{ij} is a symmetric, transverse and traceless tensor. At the quadratic order, the action governing the tensor perturbations is given by [1, 31]

$$\mathcal{S}_2[\gamma_{ij}] = \frac{M_{\text{Pl}}^2}{8} \int d\eta \int d^3\mathbf{x} \, a^2 \left[\gamma'_{ij}{}^2 - (\partial\gamma_{ij})^2 \right], \quad (3.2)$$

which, evidently, leads to a linear equation of motion. In Fourier space, the tensor modes, say, h_k , are found to satisfy the differential equation

$$h_k'' + 2 \frac{a'}{a} h_k' + k^2 h_k = 0. \quad (3.3)$$

On quantization, the tensor perturbation γ_{ij} can be decomposed in terms of the Fourier modes h_k as follows:

$$\begin{aligned} \hat{\gamma}_{ij}(\eta, \mathbf{x}) &= \int \frac{d^3\mathbf{k}}{(2\pi)^{3/2}} \hat{\gamma}_{ij}^{\mathbf{k}}(\eta) e^{i\mathbf{k}\cdot\mathbf{x}} \\ &= \sum_s \int \frac{d^3\mathbf{k}}{(2\pi)^{3/2}} \left[\hat{a}_{\mathbf{k}}^s \varepsilon_{ij}^s(\mathbf{k}) h_k(\eta) e^{i\mathbf{k}\cdot\mathbf{x}} + \hat{a}_{\mathbf{k}}^{s\dagger} \varepsilon_{ij}^{s*}(\mathbf{k}) h_k^*(\eta) e^{-i\mathbf{k}\cdot\mathbf{x}} \right], \end{aligned} \quad (3.4)$$

where the annihilation operators $\hat{a}_{\mathbf{k}}^s$ and the creation operators $\hat{a}_{\mathbf{k}}^{s\dagger}$ satisfy the standard commutation relations. The quantity $\varepsilon_{ij}^s(\mathbf{k})$ represents the polarization tensor of the gravitational waves with their helicity being denoted by the index s . The transverse and traceless nature of the gravitational waves lead to the conditions $k_i \varepsilon_{ij}^s(\mathbf{k}) = \varepsilon_{ii}^s(\mathbf{k}) = 0$. We shall choose to work with the following normalization of the polarization tensor: $\varepsilon_{ij}^r(\mathbf{k}) \varepsilon_{ij}^{s*}(\mathbf{k}) = 2\delta^{rs}$ [31].

It is often convenient to rewrite the modes h_k in terms of the corresponding Mukhanov-Sasaki variable $u_k = M_{\text{Pl}} a h_k / \sqrt{2}$. Then, the Mukhanov-Sasaki variable u_k satisfies the equation

$$u_k'' + \left(k^2 - \frac{a''}{a} \right) u_k = 0. \quad (3.5)$$

It is useful to note that the quantity a''/a can be expressed in terms of the slow roll parameter ϵ_1 as

$$\frac{a''}{a} = (aH)^2 (2 - \epsilon_1). \quad (3.6)$$

The initial conditions for the differential equation (3.5) are imposed when the modes are well inside the Hubble radius, *i.e.* when $k/(aH) \gg 1$. In this sub-Hubble limit, the following positive frequency solution of the Mukhanov-Sasaki variable u_k is chosen as the initial condition:

$$u_k(\eta) = \frac{1}{\sqrt{2k}} e^{-ik\eta}. \quad (3.7)$$

This condition is commonly referred to as the Bunch-Davies initial condition.

The tensor power spectrum, *viz.* $\mathcal{P}_T(k)$, evaluated at a suitably late conformal time, say, η_e , is defined as

$$\langle \hat{\gamma}_{ij}^{\mathbf{k}}(\eta_e) \hat{\gamma}_{mn}^{\mathbf{k}'}(\eta_e) \rangle = \frac{(2\pi)^2}{2k^3} \frac{\Pi_{ij,mn}^{\mathbf{k}}}{4} \mathcal{P}_T(k) \delta^{(3)}(\mathbf{k} + \mathbf{k}'), \quad (3.8)$$

with the expectation values on the left hand side to be evaluated in the specified initial quantum state, and the quantity $\Pi_{ij,mn}^{\mathbf{k}}$ is given by

$$\Pi_{ij,mn}^{\mathbf{k}} = \sum_s \varepsilon_{ij}^s(\mathbf{k}) \varepsilon_{mn}^{s*}(\mathbf{k}). \quad (3.9)$$

On making use of the decomposition (3.4), the inflationary tensor power spectrum evaluated in the vacuum state $|0\rangle$ (such that $\hat{a}_{\mathbf{k}}^s|0\rangle = 0 \ \forall \ \mathbf{k} \text{ and } s$) can be expressed as

$$\mathcal{P}_T(k) = 4 \frac{k^3}{2\pi^2} |h_k|^2. \quad (3.10)$$

The amplitude $|h_k|$ on the right hand side of this expression is to be evaluated when the modes are sufficiently outside the Hubble radius, *i.e.* when $k/(aH) \ll 1$. It should be mentioned here that the tensor spectral index n_T is defined as

$$n_T = \frac{d \ln \mathcal{P}_T(k)}{d \ln k}. \quad (3.11)$$

4 The tensor bispectrum and the corresponding non-Gaussianity parameter

The dominant signatures of non-Gaussianities are the three-point functions. The tensor bispectrum, *viz.* the three-point correlation function describing the tensor perturbations, that arises in a given inflationary model can be evaluated using the so-called Maldacena formalism [31]. The formalism involves first deriving the cubic order action governing the perturbations. At the cubic order, the action describing the tensor perturbations is found to be

$$S_3[\gamma_{ij}] = \frac{M_{\text{Pl}}^2}{2} \int d\eta \int d^3\mathbf{x} \left[\frac{a^2}{2} \gamma_{lj} \gamma_{im} \partial_l \partial_m \gamma_{ij} - \frac{a^2}{4} \gamma_{ij} \gamma_{lm} \partial_l \partial_m \gamma_{ij} \right]. \quad (4.1)$$

Given this action, the corresponding three-point function can then be arrived at using the standard techniques of quantum field theory. In this section, we shall gather the essential expressions describing the tensor bispectrum. We shall also define the corresponding dimensionless non-Gaussianity parameter that can be introduced for conveniently characterizing the amplitude of the tensor bispectrum, as is popularly done in the scalar case [56].

The tensor bispectrum in Fourier space, *viz.* $\mathcal{B}_{\gamma\gamma\gamma}^{m_1 n_1 m_2 n_2 m_3 n_3}(\mathbf{k}_1, \mathbf{k}_2, \mathbf{k}_3)$, evaluated towards the end of inflation at the conformal time, say, η_e , is defined as

$$\langle \hat{\gamma}_{m_1 n_1}^{\mathbf{k}_1}(\eta_e) \hat{\gamma}_{m_2 n_2}^{\mathbf{k}_2}(\eta_e) \hat{\gamma}_{m_3 n_3}^{\mathbf{k}_3}(\eta_e) \rangle = (2\pi)^3 \mathcal{B}_{\gamma\gamma\gamma}^{m_1 n_1 m_2 n_2 m_3 n_3}(\mathbf{k}_1, \mathbf{k}_2, \mathbf{k}_3) \delta^{(3)}(\mathbf{k}_1 + \mathbf{k}_2 + \mathbf{k}_3). \quad (4.2)$$

It should be mentioned that the delta function on the right hand side implies that the wavevectors \mathbf{k}_1 , \mathbf{k}_2 and \mathbf{k}_3 form the edges of a triangle. For convenience, hereafter, we shall set

$$\mathcal{B}_{\gamma\gamma\gamma}^{m_1 n_1 m_2 n_2 m_3 n_3}(\mathbf{k}_1, \mathbf{k}_2, \mathbf{k}_3) = (2\pi)^{-9/2} G_{\gamma\gamma\gamma}^{m_1 n_1 m_2 n_2 m_3 n_3}(\mathbf{k}_1, \mathbf{k}_2, \mathbf{k}_3). \quad (4.3)$$

The quantity $G_{\gamma\gamma\gamma}^{m_1 n_1 m_2 n_2 m_3 n_3}(\mathbf{k}_1, \mathbf{k}_2, \mathbf{k}_3)$, evaluated in the perturbative vacuum, can be obtained to be (see, for instance, Refs. [31, 56])

$$\begin{aligned} G_{\gamma\gamma\gamma}^{m_1 n_1 m_2 n_2 m_3 n_3}(\mathbf{k}_1, \mathbf{k}_2, \mathbf{k}_3) = & M_{\text{Pl}}^2 \left[(\Pi_{m_1 n_1, ij}^{\mathbf{k}_1} \Pi_{m_2 n_2, im}^{\mathbf{k}_2} \Pi_{m_3 n_3, lj}^{\mathbf{k}_3} \right. \\ & \left. - \frac{1}{2} \Pi_{m_1 n_1, ij}^{\mathbf{k}_1} \Pi_{m_2 n_2, ml}^{\mathbf{k}_2} \Pi_{m_3 n_3, ij}^{\mathbf{k}_3}) k_{1m} k_{1l} + \text{five permutations} \right] \\ & \times [h_{k_1}(\eta_e) h_{k_2}(\eta_e) h_{k_3}(\eta_e) \mathcal{G}_{\gamma\gamma\gamma}(\mathbf{k}_1, \mathbf{k}_2, \mathbf{k}_3) \\ & + \text{complex conjugate}], \end{aligned} \quad (4.4)$$

where $\mathcal{G}_{\gamma\gamma\gamma}(\mathbf{k}_1, \mathbf{k}_2, \mathbf{k}_3)$ is described by the integral

$$\mathcal{G}_{\gamma\gamma\gamma}(\mathbf{k}_1, \mathbf{k}_2, \mathbf{k}_3) = -\frac{i}{4} \int_{\eta_i}^{\eta_e} d\eta a^2 h_{k_1}^* h_{k_2}^* h_{k_3}^*, \quad (4.5)$$

with η_i denoting the time when the initial conditions are imposed on the perturbations.

As is well known, in the case of the scalars, a dimensionless non-Gaussianity parameter is often introduced (in fact, a set of three parameters are considered) to roughly characterize the amplitude of the scalar bispectrum. A similar dimensionless quantity can be introduced to describe the tensor bispectrum. It can be defined to be the following dimensionless ratio of the tensor bispectrum and the power spectrum [56]:

$$\begin{aligned} h_{\text{NL}}(\mathbf{k}_1, \mathbf{k}_2, \mathbf{k}_3) = & -\left(\frac{4}{2\pi^2}\right)^2 [k_1^3 k_2^3 k_3^3 G_{\gamma\gamma\gamma}^{m_1 n_1 m_2 n_2 m_3 n_3}(\mathbf{k}_1, \mathbf{k}_2, \mathbf{k}_3)] \\ & \times \left[\Pi_{m_1 n_1, m_3 n_3}^{\mathbf{k}_1} \Pi_{m_2 n_2, \bar{m} \bar{n}}^{\mathbf{k}_2} k_3^3 \mathcal{P}_{\text{T}}(k_1) \mathcal{P}_{\text{T}}(k_2) + \text{five permutations} \right]^{-1}, \end{aligned} \quad (4.6)$$

where the overbars on the indices imply that they need to be summed over all allowed values. Since we shall be focusing here only on the amplitude of the tensor bispectrum, for simplicity, we shall set the polarization tensor to unity. In such a case, the expression (4.4) for the tensor bispectrum reduces to

$$\begin{aligned} G_{\gamma\gamma\gamma}(\mathbf{k}_1, \mathbf{k}_2, \mathbf{k}_3) = & M_{\text{Pl}}^2 [h_{k_1}(\eta_e) h_{k_2}(\eta_e) h_{k_3}(\eta_e) \bar{\mathcal{G}}_{\gamma\gamma\gamma}(\mathbf{k}_1, \mathbf{k}_2, \mathbf{k}_3) \\ & + \text{complex conjugate}], \end{aligned} \quad (4.7)$$

where the quantity $\bar{\mathcal{G}}_{\gamma\gamma\gamma}(\mathbf{k}_1, \mathbf{k}_2, \mathbf{k}_3)$ is described by the integral

$$\bar{\mathcal{G}}_{\gamma\gamma\gamma}(\mathbf{k}_1, \mathbf{k}_2, \mathbf{k}_3) = -\frac{i}{4} (k_1^2 + k_2^2 + k_3^2) \int_{\eta_i}^{\eta_e} d\eta a^2 h_{k_1}^* h_{k_2}^* h_{k_3}^*. \quad (4.8)$$

Also, if we ignore the factors involving the polarization tensor, the non-Gaussianity parameter h_{NL} simplifies to

$$\begin{aligned} h_{\text{NL}}(\mathbf{k}_1, \mathbf{k}_2, \mathbf{k}_3) = & -\left(\frac{4}{2\pi^2}\right)^2 [k_1^3 k_2^3 k_3^3 G_{\gamma\gamma\gamma}(\mathbf{k}_1, \mathbf{k}_2, \mathbf{k}_3)] \\ & \times \left[2 k_3^3 \mathcal{P}_{\text{T}}(k_1) \mathcal{P}_{\text{T}}(k_2) + \text{two permutations} \right]^{-1}. \end{aligned} \quad (4.9)$$

5 The non-Gaussianity parameter h_{NL} in slow roll inflation

Evidently, in order to evaluate the tensor bispectrum, we shall first require the modes h_k . Also, using the modes, we need to be able to evaluate the integral (4.8) and the asymptotic forms of the modes to arrive at the tensor bispectrum and the corresponding non-Gaussianity parameter. In slow roll inflation, one often works in the de Sitter approximation wherein the tensor modes h_k are given by

$$h_k(\eta) = \frac{\sqrt{2} i H_0}{M_{\text{Pl}} \sqrt{2} k^3} (1 + i k \eta) e^{-i k \eta}, \quad (5.1)$$

with H_0 being the Hubble parameter in de Sitter inflation. These modes can be easily used to arrive at the following well-known, strictly scale invariant tensor power spectrum (evaluated towards the end of inflation, *i.e.* as $\eta_e \rightarrow 0$):

$$\mathcal{P}_{\text{T}}(k) = \frac{2 H_0^2}{\pi^2 M_{\text{Pl}}^2}. \quad (5.2)$$

Using the modes (5.1), the integral (4.8) can be evaluated to be

$$\bar{\mathcal{G}}_{\gamma\gamma\gamma}(\mathbf{k}_1, \mathbf{k}_2, \mathbf{k}_3) = -\frac{i H_0 (k_1^2 + k_2^2 + k_3^2)}{4 M_{\text{Pl}}^3 (k_1 k_2 k_3)^{3/2}} \left(k_{\text{T}} - \frac{k_1 k_2 + k_1 k_3 + k_2 k_3}{k_{\text{T}}} - \frac{k_1 k_2 k_3}{k_{\text{T}}^2} \right), \quad (5.3)$$

where $k_{\text{T}} = k_1 + k_2 + k_3$. In the limit $\eta_e \rightarrow 0$, the corresponding tensor bispectrum $G_{\gamma\gamma\gamma}(\mathbf{k}_1, \mathbf{k}_2, \mathbf{k}_3)$ and the non-Gaussianity parameter $h_{\text{NL}}(\mathbf{k}_1, \mathbf{k}_2, \mathbf{k}_3)$ can be obtained to be

$$G_{\gamma\gamma\gamma}(\mathbf{k}_1, \mathbf{k}_2, \mathbf{k}_3) = -\frac{H_0^4 (k_1^2 + k_2^2 + k_3^2)}{2 M_{\text{Pl}}^4 (k_1 k_2 k_3)^3} \left(k_{\text{T}} - \frac{k_1 k_2 + k_1 k_3 + k_2 k_3}{k_{\text{T}}} - \frac{k_1 k_2 k_3}{k_{\text{T}}^2} \right) \quad (5.4)$$

and

$$h_{\text{NL}}(\mathbf{k}_1, \mathbf{k}_2, \mathbf{k}_3) = \frac{1}{4} \left(\frac{k_1^2 + k_2^2 + k_3^2}{k_1^3 + k_2^3 + k_3^3} \right) \left(k_{\text{T}} - \frac{k_1 k_2 + k_2 k_3 + k_3 k_1}{k_{\text{T}}} - \frac{k_1 k_2 k_3}{k_{\text{T}}^2} \right). \quad (5.5)$$

Note that, in the equilateral limit (*i.e.* when $k_1 = k_2 = k_3$), we have $h_{\text{NL}} = 17/36 \simeq 0.472$, while in the squeezed limit (*i.e.* as $k_1 = k_2$ and $k_3 \rightarrow 0$), we have $h_{\text{NL}} = 3/8 = 0.375$. These analytical results prove to be very handy for examining the accuracy of the numerical procedures that we shall adopt to evaluate the tensor modes, the tensor power spectrum and the tensor bispectrum.

6 Numerical evaluation

As we have described before, our aim in this work is to numerically evaluate the magnitude and shape of the non-Gaussianity parameter h_{NL} in two field models of inflation. We shall make use of the analytical results available in the slow roll limit (actually, in the de Sitter limit) to check the accuracy of our numerical results. In this section, we shall first quickly describe the numerical procedure that we shall adopt for the evaluation of the non-Gaussianity parameter h_{NL} . Thereafter, we shall consider three specific inflationary models and evaluate the non-Gaussianity parameter h_{NL} in these models.

Evidently, we shall first require the behavior of the background quantities and the tensor modes. Once these are at hand, the tensor bispectrum (4.7) can be arrived at by computing the integral (4.8) and then using the asymptotic forms of the tensor modes. These quantities can be utilized to finally obtain the non-Gaussianity parameter h_{NL} .

Our numerical procedure is essentially similar to an earlier work in this context which had dealt with single field models of inflation [56]. Once the parameters in the potential and the initial conditions are specified, one can integrate the equations (2.3) that govern the scalar fields and the Friedmann equation (2.4) to arrive at the evolution of the background quantities. Usually the initial value of the fields are chosen to lead to enough number of e-folds (say, 60-70 e-folds of inflation). Once we have the background quantities, we can solve for the tensor perturbations by integrating the governing equation (3.3), along with the Bunch-Davies initial condition (3.7). In this computation, the initial conditions are imposed on the modes when they are sufficiently inside the Hubble radius [we have chosen when $k/(aH) = 10^2$]. The power spectrum is evaluated in the super-Hubble domain, when the amplitude of the modes have reached a constant value [which typically occur when $k/(aH) \simeq 10^{-5}$].

We solve the background and the perturbation equations as functions of the number of e-folds using the fifth order Runge-Kutta algorithm (see, for instance, Ref. [67]). Since the tensor mode is constant during the super Hubble evolution, we can neglect the contribution of h_{NL} during this period (for more details, see Ref. [56]). This simplifies the numerical integration involved in the calculation of h_{NL} . Note that the modes oscillate strongly in the sub-Hubble domain, leading to oscillating integrands. In order to handle such integrands, an exponential cut-off is included to regulate the integrals in the sub-Hubble domain, as has been implemented earlier in similar contexts (in this context, see Refs. [56, 57, 61]). Such a cut-off can be justified theoretically as it helps in identifying the correct perturbative vacuum [32, 58, 61]. The integration is carried out using the Bode's rule¹, from the earliest time η_i when the smallest of the three wavenumbers (k_1, k_2, k_3) is well inside the Hubble radius to the final time η_e when the largest of them is sufficiently outside the Hubble radius.

6.1 Double inflation

The simplest of two field inflationary models is the model which is described by the potential [68, 69]

$$V(\phi, \chi) = \frac{1}{2} m_\phi^2 \phi^2 + \frac{1}{2} m_\chi^2 \chi^2. \quad (6.1)$$

This model is often referred to as double inflation, since it can lead to two different epochs of inflation (characterized by different values of the Hubble parameter) if the parameters m_ϕ and m_χ are very different. Even though this model seems to be ruled out by the current observations, it is instructive to work with this model since it is very simple. As we have mentioned earlier, one of our aims is to study the effects of curved trajectories in field space on h_{NL} and, in this model, it is easy to construct different types of curved trajectories.

For numerical analysis, we shall set $m_\phi = 7.12 \times 10^{-6} M_{\text{Pl}}$, and choose m_χ to be a multiple of m_ϕ . We shall choose the initial value of the fields to be $\phi_i = 14.4 M_{\text{Pl}}$ and $\chi_i = 8.5 M_{\text{Pl}}$. The corresponding initial velocities of the fields are chosen such that the first slow roll parameter ϵ_1 is small. In Fig. 1, we have shown the trajectories of the two scalar fields and the evolution of the slow roll parameter ϵ_1 for three different mass ratios m_χ/m_ϕ . For $m_\chi = m_\phi$, the slow roll parameter ϵ_1 is very small throughout inflation, as one would

¹We should add that there is some confusion concerning whether it is Bode's or Boole's rule [67].

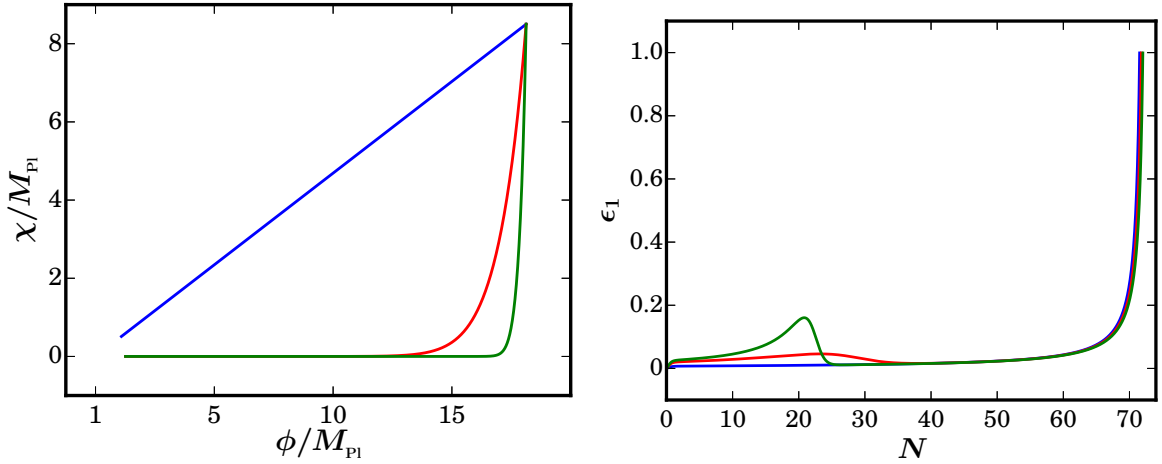


Figure 1. The trajectories of the fields ϕ and χ in the field space have been plotted (on the left) in the case of double inflation for different mass ratios $m_\chi = m_\phi$ (in blue), $m_\chi = 4m_\phi$ (in red) and $m_\chi = 8m_\phi$ (in green). The corresponding evolution of first slow roll parameter ϵ_1 has been plotted as a function of the number of e-folds (on the right) with the same choices of colors for the different cases (as in the figure on the left).

have naively expected. For $m_\chi = 4m_\phi$, the trajectory in the field space is characterized by a smooth turn from a χ dominated phase to the $\chi = 0$ valley and inflation continues along this valley. In the case of $m_\chi = 8m_\phi$, the turn is more sharp and the field reaches the $\chi = 0$ valley faster than in the former cases. It is important to note the effect of turning on the evolution of the first slow roll parameter ϵ_1 . When the mass ratio increases, the turns become sharper and the slow roll parameter ϵ_1 changes considerably during the turn.

Let us now turn to understand the behavior of the non-Gaussianity parameter in these situations. Since the case of $m_\chi = m_\phi$ leads to nearly de Sitter inflation, the numerical results for h_{NL} from this case can be compared with the analytical results we had discussed earlier. Evidently, this exercise can help us determine the accuracy of our numerical procedure. In Fig. 2, we have illustrated the density plots of h_{NL} for a triangular configuration of the wavenumbers (k_1, k_2, k_3) evaluated analytically in the case of de Sitter inflation and the numerical results for the double inflation model with equal values for the masses for the two fields. To arrive at the density plots of h_{NL} , we have set $k_1 = 5 \times 10^{-2} \text{Mpc}^{-1}$, and chosen k_2 and k_3 such that $5 \times 10^{-4} \text{Mpc}^{-1} < (k_2, k_3) < 5 \times 10^{-2} \text{Mpc}^{-1}$. Note that the non-Gaussianity parameter h_{NL} has an equilateral shape, *i.e.* its value is the largest in the equilateral limit (wherein $k_1 = k_2 = k_3$). The equilateral shape can be attributed to the fact that the non-Gaussianities are essentially generated as the modes leave the Hubble radius and the contributions on the super-Hubble scales are insignificant. This figure clearly illustrates that the numerical and the analytical results match quite well. In fact, we find that the maximum difference between them is less than 2%.

Our next task is to study the effect of the turning of the trajectory in the field space on h_{NL} , and we shall utilize the cases wherein $m_\chi = 4m_\phi$ and $m_\chi = 8m_\phi$ for this purpose. We should mention that, in these cases, the scales of our interest leave the Hubble radius between the e-folds of 16 and 33, and the direction of the trajectory changes exactly in this domain. The change in the trajectory in the field space leads to a deviation from slow roll, as

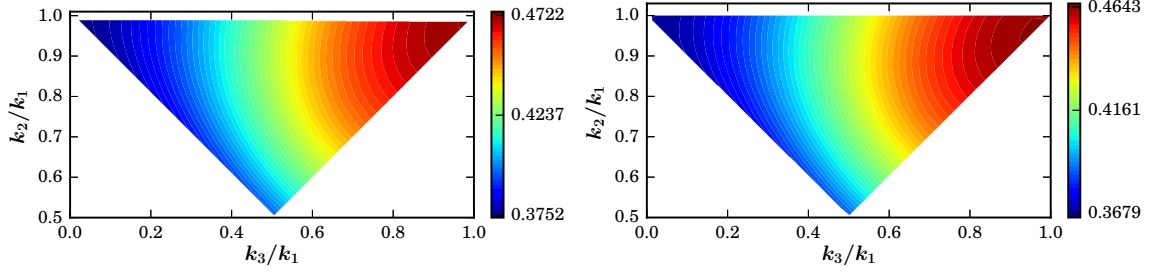


Figure 2. Density plots of h_{NL} for an arbitrary triangular configuration of the wavenumbers evaluated analytically in the case of de Sitter inflation (on the left) and obtained numerically for double inflation with $m_\chi = m_\phi$ (on the right). It is evident that the analytical and the numerical results match quite well, indicating the accuracy of the numerical procedures that have been adopted.

is evident from Fig. 1. This effects the tensor modes and the associated non-Gaussianities. In Fig. 3, we have plotted the non-Gaussianity parameter h_{NL} that arises in these two cases. While the deviation from slow roll inflation clearly modifies the amplitude of the parameter h_{NL} , the broad equilateral shape is indeed retained. The departure from slow roll boosts the amplitude of h_{NL} to a slight extent from the slow roll values. As we had mentioned, we have

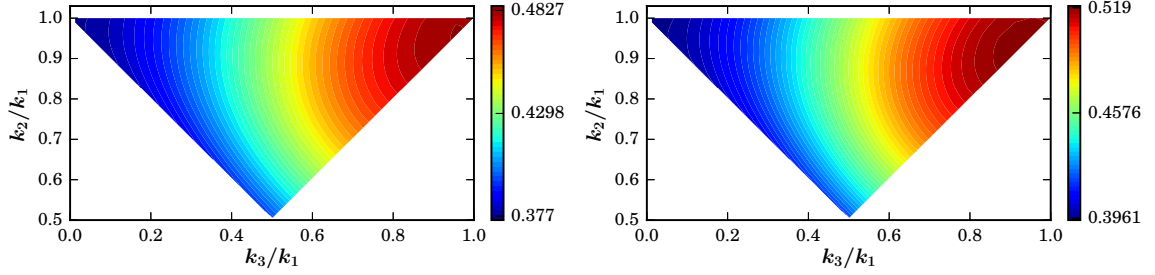


Figure 3. Density plots of h_{NL} computed numerically for an arbitrary triangular configuration of the wavenumbers for the case of double inflation with $m_\chi = 4m_\phi$ (on the left) and $m_\chi = 8m_\phi$ (on the right). Note that, in these cases, the departure from slow roll arises due to the turn in the trajectory in the field space. This deviation from slow roll enhances the amplitude of the non-Gaussianity parameter h_{NL} to some extent from the slow roll values.

considered the double inflation model because of its simplicity. In Fig. 6, we have plotted the scalar (*i.e.* the adiabatic) and the tensor power spectra that arise in these cases. Even the simpler case of $m_\phi = m_\chi$ will not be favored by the CMB data because of the large tensor-to-scalar ratio that the model leads to. (Recall that the tensor-to-scalar ratio $r \lesssim 0.1$, according to the recent Planck data [16].) The other two cases lead to a broad step-like feature in the power spectra. They also result in higher scalar power on large scales and a large tensor-to-scalar ratio. Due to these reasons, these cases are ruled out by the data as well.

In what follows, we shall discuss two more models, *viz.* hybrid inflation and aligned natural inflation. As we shall see, in these models, for the values of the parameters that we work with, the first slow roll parameter evolves smoothly and also remains very small during inflation. As a result, the non-Gaussianity parameter h_{NL} in these models does not differ

much from the case of de Sitter inflation.

6.2 Hybrid inflation

In most of the models, inflation ends when the scalar field approaches the minimum of the potential. The hybrid model of inflation had been introduced as an alternative way of ending inflation [70, 71]. In this model, inflation does not end because the field reaches a minimum, but due to a phase transition which occurs at a critical point of one of the fields. This model is based on the potential

$$V(\phi, \chi) = \frac{1}{2} m^2 \phi^2 + \frac{\lambda}{4} (\chi^2 - M^2)^2 + \frac{\lambda'}{2} \phi^2 \chi^2, \quad (6.2)$$

where λ and λ' are two positive coupling constants, while m and M represent two mass parameters. One finds that, in this model, a wide variety of trajectories are possible for different initial conditions [72, 73]. When confined to domains of sub-Planckian values for the fields, the initial values which lead to sufficient amount of e-folds are found to be near the $\chi = 0$ valley and as random points in the space of the scalar fields. But, it is observed that the initial conditions which give sufficiently long inflation can be always found in the region of super-Planckian values of the fields [72, 73].

In our analysis, we set $m = 2.63 \times 10^{-12} M_{\text{Pl}}$, $M = 4.14 \times 10^{-14} M_{\text{Pl}}$ and $\lambda = \lambda' = 2.75 \times 10^{-13}$. The scalar fields start from the initial values $\phi_i = 10.02 M_{\text{Pl}}$ and $\chi_i = 21.05 M_{\text{Pl}}$. The behavior of the slow roll parameter ϵ_1 in this model is plotted in Fig. 4, and the resulting tensor bispectrum is plotted in Fig. 5.

6.3 Aligned natural inflation

The next model we shall study is the natural inflation model with a strong alignment [74–76]. The model is described by the potential

$$V(\phi, \chi) = \Lambda^4 \left[1 - \frac{1}{1 + \beta} \cos(c_1 \alpha \phi + c_2 \chi) - \frac{\beta}{1 + \beta} \cos(c_3 \alpha \phi + c_4 \chi) \right]. \quad (6.3)$$

This model also admits different types of trajectories. But, for the values of the parameters $\Lambda = 1.76 \times 10^{-10} M_{\text{Pl}}$, $c_1 = 8.20 M_{\text{Pl}}^{-1}$, $c_2 = 12.12 M_{\text{Pl}}^{-1}$, $c_3 = 8.80 M_{\text{Pl}}^{-1}$, $c_4 = 27.27 M_{\text{Pl}}^{-1}$, $\alpha = 0.01$ and $\beta = 0.41$, the initial conditions $\phi_i = 24.2 M_{\text{Pl}}$ and $\chi_i = -0.1 M_{\text{Pl}}$, lead to a special kind of trajectory in which inflation ends due to the instability in the direction of the heavy field. This trajectory is interesting due to the fact that it leads to a suppressed value for the tensor-to-scalar ratio. The first slow roll parameter is very small throughout inflation and it undergoes an extremely sharp change in its value to end inflation (cf. Fig. 4). We shall make use of this trajectory for evaluating h_{NL} .

From Fig. 4, it is clear that in both the models (*i.e.* the hybrid inflation model and the aligned natural inflation model), the slow roll parameter ϵ_1 remains very small throughout inflation. So, we do not expect much change in the value of h_{NL} from the case of de Sitter inflation and this expectation is confirmed by Fig. 5. For the sake of completeness we have included the plots of the scalar and tensor power spectra that arise in these models in Fig. 6.

For the values of the parameters we have worked with, the hybrid inflation model seems to lead to a rather high tensor-to-scalar ratio, and hence it is likely to be ruled out by the data. In contrast, as we had mentioned, the aligned natural inflation model results in a considerably suppressed tensor-to-scalar ratio and, therefore, it can be expected to be consistent with the data.

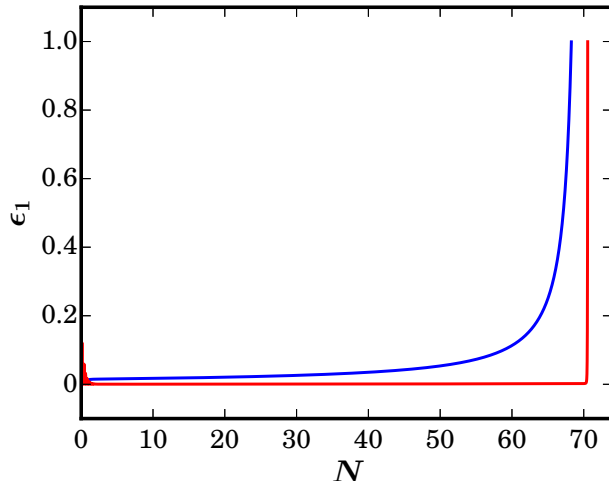


Figure 4. The evolution of first slow roll parameter ϵ_1 in the case of hybrid inflation (in blue) and aligned natural inflation (in red).

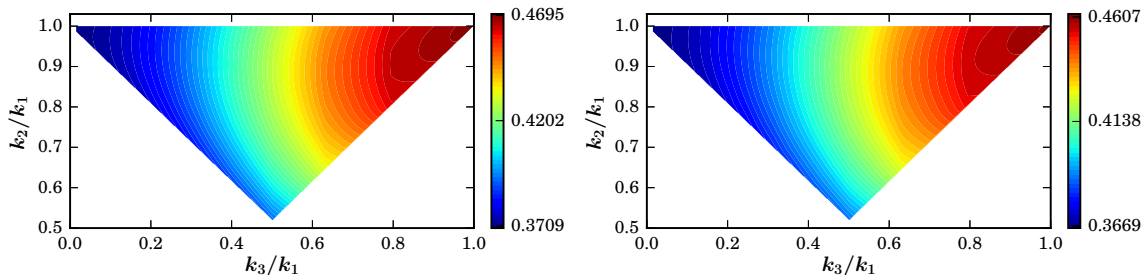


Figure 5. Density plots of the non-Gaussianity parameter h_{NL} evaluated numerically for an arbitrary triangular configuration of the wavenumbers for the case of hybrid inflation (on the left) and aligned natural inflation (on the right).

7 Consistency relation in the squeezed limit

It is well known that the amplitude of the tensor perturbations freeze on super-Hubble scales. Due to this reason, if one considers the long wavelength limit of one of the wavenumbers (often referred to as the squeezed limit), it can be shown that the tensor bispectrum can be completely expressed in terms of the tensor power spectrum. Specifically, if we choose $k_3 \rightarrow 0$ so that $k_2 \simeq k_3 = k$, one finds that the non-Gaussianity parameter h_{NL} can be expressed as follows [62]:

$$\lim_{k_3 \rightarrow 0} h_{\text{NL}}(\mathbf{k}, -\mathbf{k}, \mathbf{k}_3) = \frac{n_{\text{T}}(k) - 3}{8}, \quad (7.1)$$

where n_{T} is the tensor spectral index defined as in Eq. (3.11). Since we have been able to evaluate the non-Gaussianity parameter h_{NL} (and the spectral index n_{T}) for an arbitrary triangular configuration of the wavenumbers, it is interesting to examine if the above consistency is indeed satisfied in the models we have considered. In Fig. 7, we have plotted these two quantities for the double inflation model with $m_\chi = 8m_\phi$, which leads to the

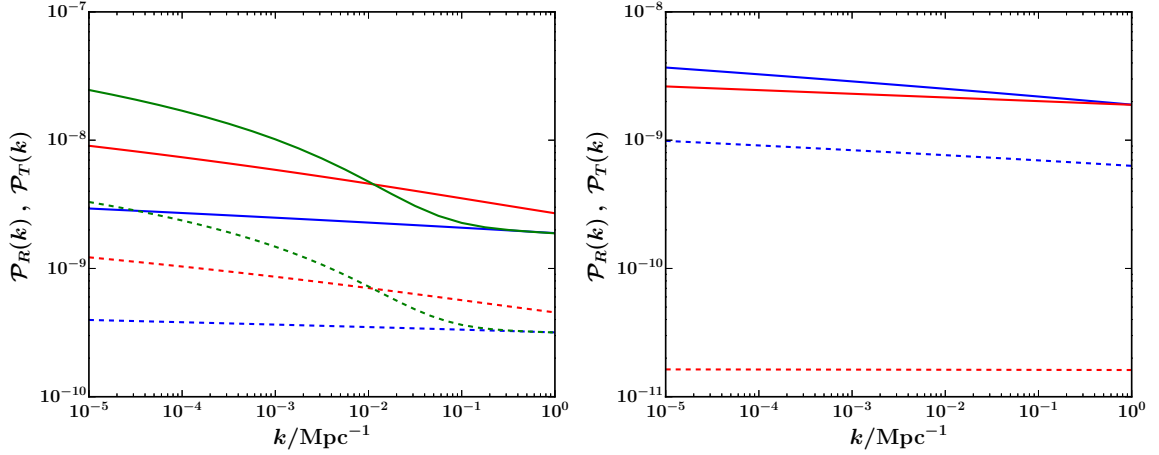


Figure 6. The scalar, *i.e.* adiabatic (solid line) and the tensor (dashed line) power spectra have been plotted (on the left) for the double inflation model with $m_\chi = m_\phi$ (in blue), $m_\chi = 4 m_\phi$ (in red) and $m_\chi = 8 m_\phi$ (in green). The power spectra (with same choice of lines) have also been plotted (on the right) for the cases of the hybrid inflation (in blue) and the aligned natural inflation (in red) models.

maximum possible deviation from slow roll. We find that the maximum difference between

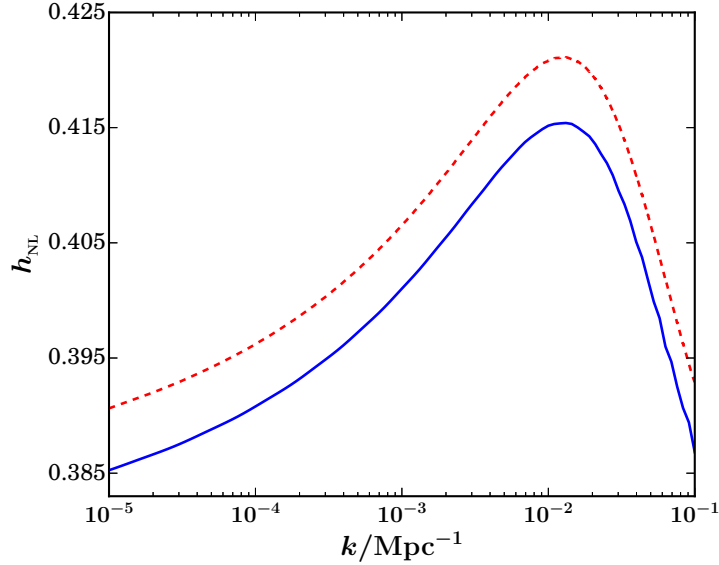


Figure 7. The non-Gaussianity parameter h_{NL} evaluated numerically in the squeezed limit (the solid line) and the quantity $(n_{\text{T}} - 3)/8$ obtained from the tensor power spectrum (the dashed line) have been plotted in the case of the double inflation model wherein $m_\chi = 8 m_\phi$. The maximum difference between these quantities is about 1.2% and the difference can be attributed to the level of numerical accuracy that one has worked with. This suggests that the consistency relation is valid even away from slow roll.

these quantities evaluated numerically is about 1.2%, which clearly supports the validity of

the consistency relation even in situations involving departures from slow roll.

8 The contribution during preheating

In models such as double inflation, the scalar field rolls down the potential and inflation is terminated when the field is close to the minimum of the potential. After inflation has ended, the scalar field oscillates about the minimum of the potential, a phase which is referred to as preheating. Note that all perturbations of cosmological interest are on super-Hubble scales during the domain of preheating. Due to this reason, the oscillations in the scalar field are not expected to affect the evolution of the amplitude of h_k , which remain constant as in the super-Hubble domain during inflation. We have evolved the tensor perturbations numerically through the epoch of preheating. In Fig. 8, we have plotted the evolution of the amplitude of h_k (for a specific mode) in the case of the double inflation model during the epochs of inflation and preheating. Clearly, the figure corroborates the expectation that the amplitude of h_k is constant at suitably late times. Since the amplitude of the tensor modes is constant, the

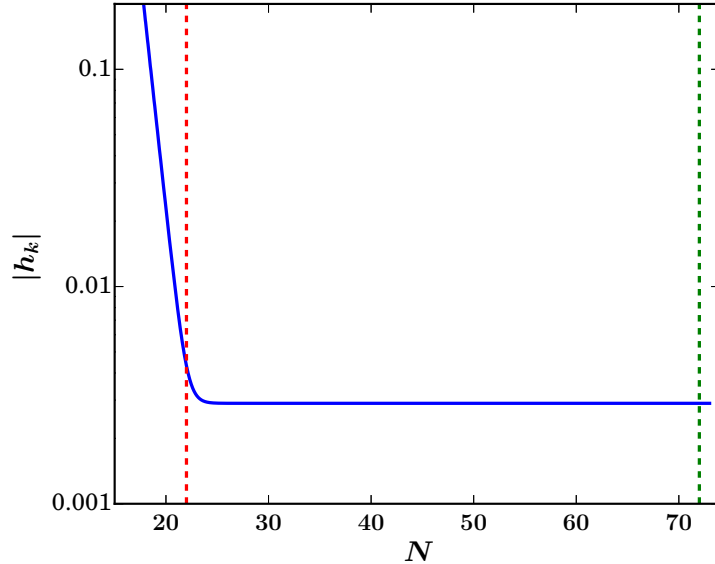


Figure 8. Evolution of the absolute value of h_k for $k = 0.05 \text{ Mpc}^{-1}$ during the epochs of inflation and reheating in the case of the double inflation model with $m_\chi = 8 m_\phi$. The vertical red and green lines indicate the time when the mode leaves the Hubble radius during inflation and the end of inflation, respectively.

contribution to the non-Gaussianity parameter h_{NL} due to this epoch is identically zero [56].

9 Discussion

As we have stressed earlier, primordial non-Gaussianities are expected to provide crucial information to help us arrive at stronger constraints on the physics of the early universe. Apart from the very recent efforts, there has been little work towards the numerical evaluation of non-Gaussianities in multi field models of inflation. As a preliminary step, in this work, we have evaluated the tensor bispectrum in two field models of inflation. We have been able

to compare the numerical results with the analytical results available in the case of slow roll inflation. This comparison suggests that the numerical procedure we have adopted is quite accurate. The two field models are interesting because of the curved trajectories that can be generated in the field space in a rather simple manner. One of our aims was to identify the effect of such a turn in the trajectory on the magnitude and the shape of h_{NL} . In double inflation, we have found that the change in the direction of the trajectory produces a bump in the first slow roll parameter, which increases the amplitude of h_{NL} over a certain domain. We have also studied the behavior of h_{NL} in the case of hybrid inflation and aligned natural inflation. Lastly, we have shown that the contribution to h_{NL} due to the epoch of preheating can be completely neglected, due to the constant amplitude of the tensor modes during this period.

Evaluating the tensor bispectrum has proved to be simpler since the evolution of the tensor modes depend only on the behavior of the scale factor. Moreover, the fact the tensor modes freeze on super-Hubble scales makes the computation easier. We are presently extending our code to evaluate the other three-point functions in two field models. In the case of the three-point functions involving scalars, the presence of iso-curvature perturbations provides a challenge, as they can lead to non-trivial evolution of the curvature perturbation on super-Hubble scales. We are currently working on this issue.

Acknowledgements

We wish to thank Debika Chowdhury for comments on the manuscript. LS wishes to thank the Indian Institute of Technology Madras, Chennai, India, for support through the New Faculty Seed Grant.

References

- [1] V. F. Mukhanov, H. A. Feldman, and R. H. Brandenberger, *Theory of cosmological perturbations*, *Physics Reports* **215** (1992), no. 5 203–333.
- [2] J. Martin, *Inflation and precision cosmology*, *Braz. J. Phys.* **34** (2004) 1307–1321, [[astro-ph/0312492](#)].
- [3] B. A. Bassett, S. Tsujikawa, and D. Wands, *Inflation dynamics and reheating*, *Rev. Mod. Phys.* **78** (May, 2006) 537–589.
- [4] L. Sriramkumar, *An introduction to inflation and cosmological perturbation theory*, [arXiv:0904.4584](#).
- [5] D. Baumann, *Inflation*, in *Physics of the large and the small, TASI 09, proceedings of the Theoretical Advanced Study Institute in Elementary Particle Physics, Boulder, Colorado, USA, 1-26 June 2009*, pp. 523–686, 2011. [arXiv:0907.5424](#).
- [6] L. Sriramkumar, *On the generation and evolution of perturbations during inflation and reheating*, in *Vignettes in Gravitation and Cosmology* (L. Sriramkumar and T. Seshadri, eds.), pp. 207–249. World Scientific, Singapore, 2012.
- [7] J. Martin, *The Observational Status of Cosmic Inflation after Planck*, *Astrophys. Space Sci. Proc.* **45** (2016) 41–134, [[arXiv:1502.05733](#)].
- [8] M. J. Mortonson, H. V. Peiris, and R. Easther, *Bayesian Analysis of Inflation: Parameter Estimation for Single Field Models*, *Phys. Rev.* **D83** (2011) 043505, [[arXiv:1007.4205](#)].
- [9] R. Easther and H. V. Peiris, *Bayesian Analysis of Inflation II: Model Selection and Constraints on Reheating*, *Phys. Rev.* **D85** (2012) 103533, [[arXiv:1112.0326](#)].

- [10] J. Norena, C. Wagner, L. Verde, H. V. Peiris, and R. Easther, *Bayesian Analysis of Inflation III: Slow Roll Reconstruction Using Model Selection*, *Phys. Rev.* **D86** (2012) 023505, [[arXiv:1202.0304](#)].
- [11] J. Martin, C. Ringeval, and R. Trotta, *Hunting Down the Best Model of Inflation with Bayesian Evidence*, *Phys. Rev.* **D83** (2011) 063524, [[arXiv:1009.4157](#)].
- [12] J. Martin, C. Ringeval, and V. Vennin, *Encyclopædia Inflationaris*, *Phys. Dark Univ.* **5-6** (2014) 75–235, [[arXiv:1303.3787](#)].
- [13] J. Martin, C. Ringeval, R. Trotta, and V. Vennin, *The Best Inflationary Models After Planck*, *JCAP* **1403** (2014) 039, [[arXiv:1312.3529](#)].
- [14] J. Martin, C. Ringeval, R. Trotta, and V. Vennin, *Compatibility of Planck and BICEP2 in the Light of Inflation*, *Phys. Rev.* **D90** (2014), no. 6 063501, [[arXiv:1405.7272](#)].
- [15] J. Martin, C. Ringeval, and V. Vennin, *How Well Can Future CMB Missions Constrain Cosmic Inflation?*, *JCAP* **1410** (2014), no. 10 038, [[arXiv:1407.4034](#)].
- [16] **Planck** Collaboration, P. A. R. Ade et al., *Planck 2015 results. XX. Constraints on inflation*, [arXiv:1502.02114](#).
- [17] S. Tsujikawa, D. Parkinson, and B. A. Bassett, *Correlation - consistency cartography of the double inflation landscape*, *Phys. Rev.* **D67** (2003) 083516, [[astro-ph/0210322](#)].
- [18] D. Parkinson, S. Tsujikawa, B. A. Bassett, and L. Amendola, *Testing for double inflation with WMAP*, *Phys. Rev.* **D71** (2005) 063524, [[astro-ph/0409071](#)].
- [19] R. Easther, J. Frazer, H. V. Peiris, and L. C. Price, *Simple predictions from multifield inflationary models*, *Phys. Rev. Lett.* **112** (2014) 161302, [[arXiv:1312.4035](#)].
- [20] D. Polarski, *Spectrum of scalar (adiabatic) perturbations in a model of double inflation*, *Phys. Rev.* **D49** (1994) 6319–6326.
- [21] D. Langlois, *Correlated adiabatic and isocurvature perturbations from double inflation*, *Phys. Rev.* **D59** (1999) 123512, [[astro-ph/9906080](#)].
- [22] C. Gordon, D. Wands, B. A. Bassett, and R. Maartens, *Adiabatic and entropy perturbations from inflation*, *Phys. Rev.* **D63** (2001) 023506, [[astro-ph/0009131](#)].
- [23] N. Bartolo, S. Matarrese, and A. Riotto, *Adiabatic and isocurvature perturbations from inflation: Power spectra and consistency relations*, *Phys. Rev.* **D64** (2001) 123504, [[astro-ph/0107502](#)].
- [24] C. T. Byrnes and D. Wands, *Curvature and isocurvature perturbations from two-field inflation in a slow-roll expansion*, *Phys. Rev.* **D74** (2006) 043529, [[astro-ph/0605679](#)].
- [25] Z. Lalak, D. Langlois, S. Pokorski, and K. Turzynski, *Curvature and isocurvature perturbations in two-field inflation*, *JCAP* **0707** (2007) 014, [[arXiv:0704.0212](#)].
- [26] D. Langlois and S. Renaux-Petel, *Perturbations in generalized multi-field inflation*, *JCAP* **0804** (2008) 017, [[arXiv:0801.1085](#)].
- [27] D. Wands, *Multiple field inflation*, *Lect. Notes Phys.* **738** (2008) 275–304, [[astro-ph/0702187](#)].
- [28] D. Langlois, *Lectures on inflation and cosmological perturbations*, *Lect. Notes Phys.* **800** (2010) 1–57, [[arXiv:1001.5259](#)].
- [29] J.-O. Gong, *Multi-field inflation and cosmological perturbations*, [arXiv:1606.06971](#).
- [30] **Planck** Collaboration, P. A. R. Ade et al., *Planck 2013 Results. XXIV. Constraints on primordial non-Gaussianity*, *Astron. Astrophys.* **571** (2014) A24, [[arXiv:1303.5084](#)].
- [31] J. M. Maldacena, *Non-Gaussian features of primordial fluctuations in single field inflationary models*, *JHEP* **05** (2003) 013, [[astro-ph/0210603](#)].

- [32] D. Seery and J. E. Lidsey, *Primordial non-Gaussianities in single field inflation*, *JCAP* **0506** (2005) 003, [[astro-ph/0503692](#)].
- [33] X. Chen, *Running non-Gaussianities in DBI inflation*, *Phys. Rev.* **D72** (2005) 123518, [[astro-ph/0507053](#)].
- [34] X. Chen, M.-x. Huang, S. Kachru, and G. Shiu, *Observational signatures and non-Gaussianities of general single field inflation*, *JCAP* **0701** (2007) 002, [[hep-th/0605045](#)].
- [35] D. Langlois, S. Renaux-Petel, D. A. Steer, and T. Tanaka, *Primordial fluctuations and non-Gaussianities in multi-field DBI inflation*, *Phys. Rev. Lett.* **101** (2008) 061301, [[arXiv:0804.3139](#)].
- [36] D. Langlois, S. Renaux-Petel, D. A. Steer, and T. Tanaka, *Primordial perturbations and non-Gaussianities in DBI and general multi-field inflation*, *Phys. Rev.* **D78** (2008) 063523, [[arXiv:0806.0336](#)].
- [37] X. Chen, *Primordial Non-Gaussianities from Inflation Models*, *Adv. Astron.* **2010** (2010) 638979, [[arXiv:1002.1416](#)].
- [38] Y. Wang, *Inflation, Cosmic Perturbations and Non-Gaussianities*, *Commun.Theor.Phys.* **62** (2014) 109–166, [[arXiv:1303.1523](#)].
- [39] E. Komatsu and D. N. Spergel, *Acoustic signatures in the primary microwave background bispectrum*, *Phys. Rev.* **D63** (2001) 063002, [[astro-ph/0005036](#)].
- [40] E. Komatsu, D. N. Spergel, and B. D. Wandelt, *Measuring primordial non-Gaussianity in the cosmic microwave background*, *Astrophys. J.* **634** (2005) 14–19, [[astro-ph/0305189](#)].
- [41] D. Babich and M. Zaldarriaga, *Primordial bispectrum information from CMB polarization*, *Phys. Rev.* **D70** (2004) 083005, [[astro-ph/0408455](#)].
- [42] M. Liguori, F. K. Hansen, E. Komatsu, S. Matarrese, and A. Riotto, *Testing primordial non-gaussianity in cmb anisotropies*, *Phys. Rev.* **D73** (2006) 043505, [[astro-ph/0509098](#)].
- [43] C. Hikage, E. Komatsu, and T. Matsubara, *Primordial Non-Gaussianity and Analytical Formula for Minkowski Functionals of the Cosmic Microwave Background and Large-scale Structure*, *Astrophys. J.* **653** (2006) 11–26, [[astro-ph/0607284](#)].
- [44] J. R. Fergusson and E. P. S. Shellard, *Primordial non-Gaussianity and the CMB bispectrum*, *Phys. Rev.* **D76** (2007) 083523, [[astro-ph/0612713](#)].
- [45] A. P. S. Yadav, E. Komatsu, and B. D. Wandelt, *Fast Estimator of Primordial Non-Gaussianity from Temperature and Polarization Anisotropies in the Cosmic Microwave Background*, *Astrophys. J.* **664** (2007) 680–686, [[astro-ph/0701921](#)].
- [46] P. Creminelli, L. Senatore, and M. Zaldarriaga, *Estimators for local non-Gaussianities*, *JCAP* **0703** (2007) 019, [[astro-ph/0606001](#)].
- [47] A. P. S. Yadav and B. D. Wandelt, *Evidence of Primordial Non-Gaussianity (f_{NL}) in the Wilkinson Microwave Anisotropy Probe 3-Year Data at 2.8sigma*, *Phys. Rev. Lett.* **100** (2008) 181301, [[arXiv:0712.1148](#)].
- [48] C. Hikage, T. Matsubara, P. Coles, M. Liguori, F. K. Hansen, and S. Matarrese, *Limits on Primordial Non-Gaussianity from Minkowski Functionals of the WMAP Temperature Anisotropies*, *Mon. Not. Roy. Astron. Soc.* **389** (2008) 1439–1446, [[arXiv:0802.3677](#)].
- [49] O. Rudjord, F. K. Hansen, X. Lan, M. Liguori, D. Marinucci, and S. Matarrese, *An Estimate of the Primordial Non-Gaussianity Parameter f_{NL} Using the Needlet Bispectrum from WMAP*, *Astrophys. J.* **701** (2009) 369–376, [[arXiv:0901.3154](#)].
- [50] K. M. Smith, L. Senatore, and M. Zaldarriaga, *Optimal limits on f_{NL}^{local} from WMAP 5-year data*, *JCAP* **0909** (2009) 006, [[arXiv:0901.2572](#)].

- [51] J. Smidt, A. Amblard, C. T. Byrnes, A. Cooray, A. Heavens, and D. Munshi, *CMB Constraints on Primordial non-Gaussianity from the Bispectrum (f_{NL}) and Trispectrum (g_{NL} and τ_{NL}) and a New Consistency Test of Single-Field Inflation*, *Phys. Rev.* **D81** (2010) 123007, [[arXiv:1004.1409](#)].
- [52] J. R. Fergusson, M. Liguori, and E. P. S. Shellard, *The CMB Bispectrum*, *JCAP* **1212** (2012) 032, [[arXiv:1006.1642](#)].
- [53] J. M. Maldacena and G. L. Pimentel, *On graviton non-Gaussianities during inflation*, *JHEP* **09** (2011) 045, [[arXiv:1104.2846](#)].
- [54] X. Gao, T. Kobayashi, M. Yamaguchi, and J. Yokoyama, *Primordial non-Gaussianities of gravitational waves in the most general single-field inflation model*, *Phys. Rev. Lett.* **107** (2011) 211301, [[arXiv:1108.3513](#)].
- [55] X. Gao, T. Kobayashi, M. Shiraishi, M. Yamaguchi, J. Yokoyama, and S. Yokoyama, *Full bispectra from primordial scalar and tensor perturbations in the most general single-field inflation model*, *PTEP* **2013** (2013) 053E03, [[arXiv:1207.0588](#)].
- [56] V. Sreenath, R. Tibrewala, and L. Sriramkumar, *Numerical evaluation of the three-point scalar-tensor cross-correlations and the tensor bi-spectrum*, *JCAP* **1312** (2013) 037, [[arXiv:1309.7169](#)].
- [57] X. Chen, R. Easther, and E. A. Lim, *Large Non-Gaussianities in Single Field Inflation*, *JCAP* **0706** (2007) 023, [[astro-ph/0611645](#)].
- [58] X. Chen, R. Easther, and E. A. Lim, *Generation and Characterization of Large Non-Gaussianities in Single Field Inflation*, *JCAP* **0804** (2008) 010, [[arXiv:0801.3295](#)].
- [59] P. Adshead, W. Hu, C. Dvorkin, and H. V. Peiris, *Fast Computation of Bispectrum Features with Generalized Slow Roll*, *Phys. Rev.* **D84** (2011) 043519, [[arXiv:1102.3435](#)].
- [60] P. Adshead, C. Dvorkin, W. Hu, and E. A. Lim, *Non-Gaussianity from Step Features in the Inflationary Potential*, *Phys. Rev.* **D85** (2012) 023531, [[arXiv:1110.3050](#)].
- [61] D. K. Hazra, L. Sriramkumar, and J. Martin, *BINGO: A code for the efficient computation of the scalar bi-spectrum*, *JCAP* **1305** (2013) 026, [[arXiv:1201.0926](#)].
- [62] V. Sreenath and L. Sriramkumar, *Examining the consistency relations describing the three-point functions involving tensors*, *JCAP* **1410** (2014), no. 10 021, [[arXiv:1406.1609](#)].
- [63] V. Sreenath, D. K. Hazra, and L. Sriramkumar, *On the scalar consistency relation away from slow roll*, *JCAP* **1502** (2015), no. 02 029, [[arXiv:1410.0252](#)].
- [64] M. Dias, J. Frazer, D. J. Mulryne, and D. Seery, *Numerical evaluation of the bispectrum in multiple field inflation*, [[arXiv:1609.00379](#)].
- [65] D. Seery, *C++Transport: a platform to automate calculation of inflationary correlation functions*, [[arXiv:1609.00380](#)].
- [66] D. J. Mulryne, *PyTransport: A Python package for the calculation of inflationary correlation functions*, [[arXiv:1609.00381](#)].
- [67] W. H. Press, S. A. Teukolsky, W. T. Vetterling, and B. P. Flannery, *Numerical Recipes 3rd Edition: The Art of Scientific Computing*. Cambridge University Press, New York, NY, USA, 3 ed., 2007.
- [68] J. Silk and M. S. Turner, *Double Inflation*, *Phys. Rev.* **D35** (1987) 419.
- [69] R. Holman, E. W. Kolb, S. L. Vadas, and Y. Wang, *Plausible double inflation*, *Phys. Lett.* **B269** (1991) 252–256.
- [70] A. D. Linde, *Hybrid inflation*, *Phys. Rev.* **D49** (1994) 748–754, [[astro-ph/9307002](#)].
- [71] D. H. Lyth and E. D. Stewart, *More varieties of hybrid inflation*, *Phys. Rev.* **D54** (1996)

7186–7190, [[hep-ph/9606412](#)].

- [72] S. Clesse and J. Rocher, *Avoiding the blue spectrum and the fine-tuning of initial conditions in hybrid inflation*, *Phys. Rev.* **D79** (2009) 103507, [[arXiv:0809.4355](#)].
- [73] S. Clesse, C. Ringeval, and J. Rocher, *Fractal initial conditions and natural parameter values in hybrid inflation*, *Phys. Rev.* **D80** (2009) 123534, [[arXiv:0909.0402](#)].
- [74] C. Long, L. McAllister, and P. McGuirk, *Aligned Natural Inflation in String Theory*, *Phys. Rev.* **D90** (2014) 023501, [[arXiv:1404.7852](#)].
- [75] R. Kappl, S. Krippendorff, and H. P. Nilles, *Aligned Natural Inflation: Monodromies of two Axions*, *Phys. Lett.* **B737** (2014) 124–128, [[arXiv:1404.7127](#)].
- [76] M. Peloso and C. Unal, *Trajectories with suppressed tensor-to-scalar ratio in Aligned Natural Inflation*, *JCAP* **1506** (2015), no. 06 040, [[arXiv:1504.02784](#)].